Combined Sensitivity Analysis of Hypersonic Aerothermodynamics to Meshing and Solver

An Undergraduate Honors Thesis

Submitted to the Department of Mechanical and Aerospace Engineering

The Ohio State University

In The Partial Fulfillment of the Requirements

For Graduation with Honors Research Distinction in Aerospace Engineering

Kaitlyn E Minsavage

Advisor: Dr Jack McNamara

April 2019

Abstract

Difficulty in experimental study and limited flight test data makes computational fluid dynamics (CFD) a critical tool in understanding the hypersonic flow regime. Key factors influencing predictive accuracy are the computational grid configuration and the solver used. A sensitivity study is conducted by varying: 1) grid type (unstructured vs. structured), 2) mesh resolution, and 3) CFD solver (ANSYS Fluent vs. NASA Langley FUN3D). The differences are highlighted by considering a simple configuration, namely a double-wedge airfoil. Metrics for comparison include inviscid and viscous pressure profiles, inviscid and adiabatic wall temperature, and heat flux profile over an isothermal wall at 300K. No strong sensitivity is observed for mesh configuration or solver for the pressure in inviscid flow. Furthermore, numerical and theoretical predictions are in close agreement. Notable deviations are observed for viscous flow, particularly between the two solvers. This is most evident in terms of adiabatic wall temperature and heat flux distributions.

Acknowledgements

I'd like to thank everyone who I worked alongside as part of MIRG for providing support, advice, and snacks. Special thanks to Dr. Ben Grier and Emily Dreyer for their assistance with this project.

Dr. McNamara and Dr. Chen, for agreeing to be part of my defense committee.

To my fiancé Charles: I wouldn't have been able to do this without you.

Table of Contents

List of Figures

List of Tables

Chapter 1: Introduction

1.1 Background

Hypersonic flight has long stood as a challenge to the engineering world. In these high energy environments, many assumptions that are commonly used at lower speeds fall apart. For example, air is frequently treated as a continuous, homogenous fluid, but in the high temperature environment it has been known to dissociate [1].

With the failure of many assumptions, there is a lack of analytical solutions to hypersonic flow problems. Additionally, hypersonic environments are extremely difficult and expensive to replicate experimentally [2]. As hypersonic flow only occurs naturally upon meteor entry into the atmosphere [1], there is also a lack of flight data that might be used to develop empirical relations.

Despite these challenges, achieving sustained hypersonic flight is still a goal of many aerospace programs. Computational fluid dynamics, or CFD, is a commonly used tool that, at its best, fills in the gaps in the knowledge and understanding regarding the flow field around a vehicle.

CFD concerns the solving of the governing equations of the flow. The partial differential equations are discretized so that they can be converted to algebraic equations that can then be solved with computers. The flow field surrounding the vehicle is discretized into a grid, of which there are two main types; unstructured and structured.

Structured grids frequently resemble grid-paper that has been stretched and twisted so that the edges align with the edges of the vehicle. Cells are ordered in a logical structured; the neighbors to cell with indices of (i,j) are (i+1, j), (i-1, j), (i,j+1), etc. In contrast, unstructured grids are far more arbitrary, where neighboring cells may not necessarily have consecutive indices. Unstructured grids also allow for more options with respect to cell shape, as both the quadrilaterals seen in structured meshes and triangular cells can be used.

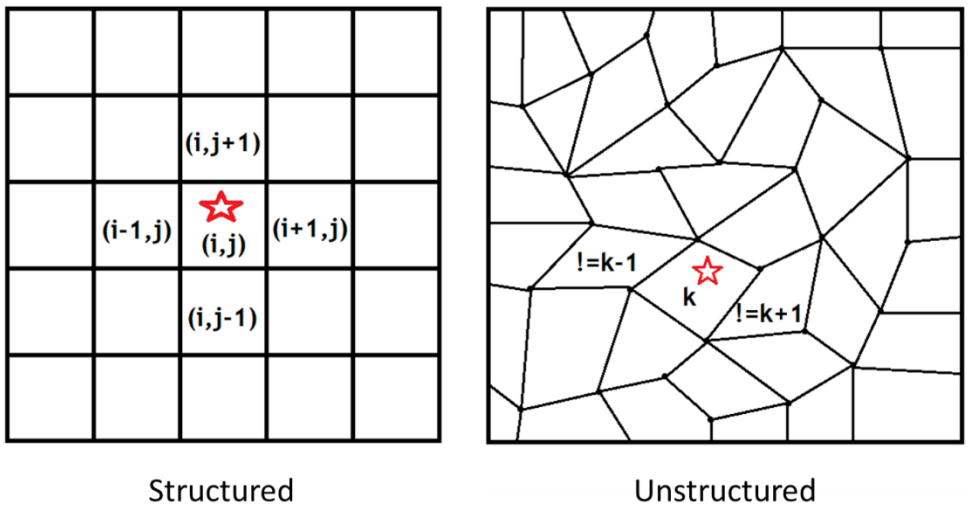

Figure 1:Example of structured and unstructured meshes for a square domain

These differences in grids can lead to differing results. However, there is not a general set of rules that can be applied to all CFD situations that lead to reliable results. For example, the quantities that seek to be studied may influence the level of refinement that is necessary for the grid to generate usable results. Additionally, different programs may solve the governing equations differently and produce differing results.

Ansys Fluent is one such CFD program. It is a commercially developed software that is used both for industry applications and academic research. Likewise, NASA Langley's FUN3D is also used for academic and government research. Both solvers treat any mesh, regardless of it was originally defined, as an unstructured mesh. For a simple geometry, such as flow over a double-wedge airfoil, it is believed that the solvers would produce comparable results.

1.2 Significance of Research

The extreme pressure and thermal loading that hypersonic vehicles experience heavily influence their design. Therefore, it is crucial to perform CFD analyses for a proposed vehicle such that the effects of the flow environment are properly accounted for. However, the lack of rules regarding meshing introduces a costly and time-consuming iterative process where results are generated with increasingly refined meshes. This research projects seeks to evaluate how three different variables relate to the predictive accuracy of CFD results: mesh density, mesh type, and solver.

1.3 Overview of Thesis

A sensitivity study will be conducted with regards to mesh type, density, and solver for the simple geometry of a double-wedge airfoil at Mach 16. Six meshes will be generated: a structured and unstructured mesh for three levels of refinement. All mesh types and refinement levels will be used with Ansys Fluent, while only the finest meshes will be used with FUN3D. Three cases will be studied: inviscid flow, viscous flow over an adiabatic wall, and viscous flow over an isothermal wall at 300K. The results will be compared to theoretical values where they exist; elsewise, agreement between the solvers will be sought to evaluate the results.

Chapter 2: Methodology

Three cases will be considered: an idealized, inviscid case; an extreme, adiabatic wall case; and a realistic case with an isothermal wall temperature of 300K. All meshes will be used for each case in Fluent, while only the finest meshes will be used with FUN3D. Boundary conditions will be consistent with those of standard atmospheric conditions at 40,000 ft. For viscous cases, the Spallart-Allarmas turbulence model will be used.

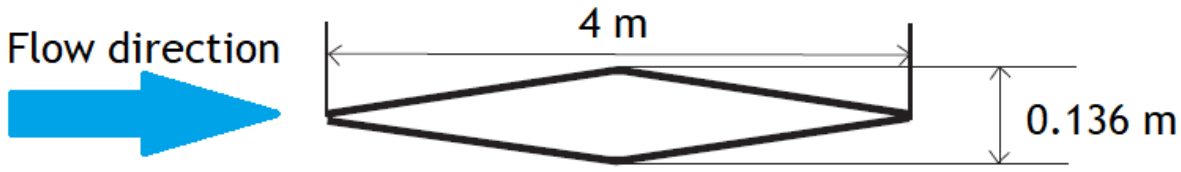

Figure 2: Schematic of geometry considered

2.1 Inviscid Comparison

The inviscid case represents an extremely simplified scenario that will not be realized during atmospheric flight. This case assumes no viscous effects, which allows an analytical solution to be derived from shock-expansion theory. The flow properties over the airfoil obtained from the CFD solvers will be compared against this analytical solution. Additionally, the coefficient of drag will be used as a nondimensional metric to evaluate the meshes and solvers.

2.2 Adiabatic Comparison

The wall of the airfoil will have an adiabatic thermal boundary condition prescribed. This represents an extreme, as the temperatures necessary to the achieve an adiabatic wall are extremely high and cannot be supported by the structured. However, it will provide a comparison, particularly between the CFD solvers, regarding how thermal boundary conditions are enforced. Comparisons will be made between the pressure and temperature distributions across the airfoil for the adiabatic case. The coefficient of drag will be used to nondimensionally compare the results.

2.3 Wall Temperature at 300K

The wall temperature of the airfoil will be set to more realistic value of 300K in order to produce a heat flux. Pressures across the airfoil and the coefficient of drag will be compared.

Chapter 3: Results

Six meshes were generated to be used in this project; three levels of refinement were used with both structured and unstructured meshes.

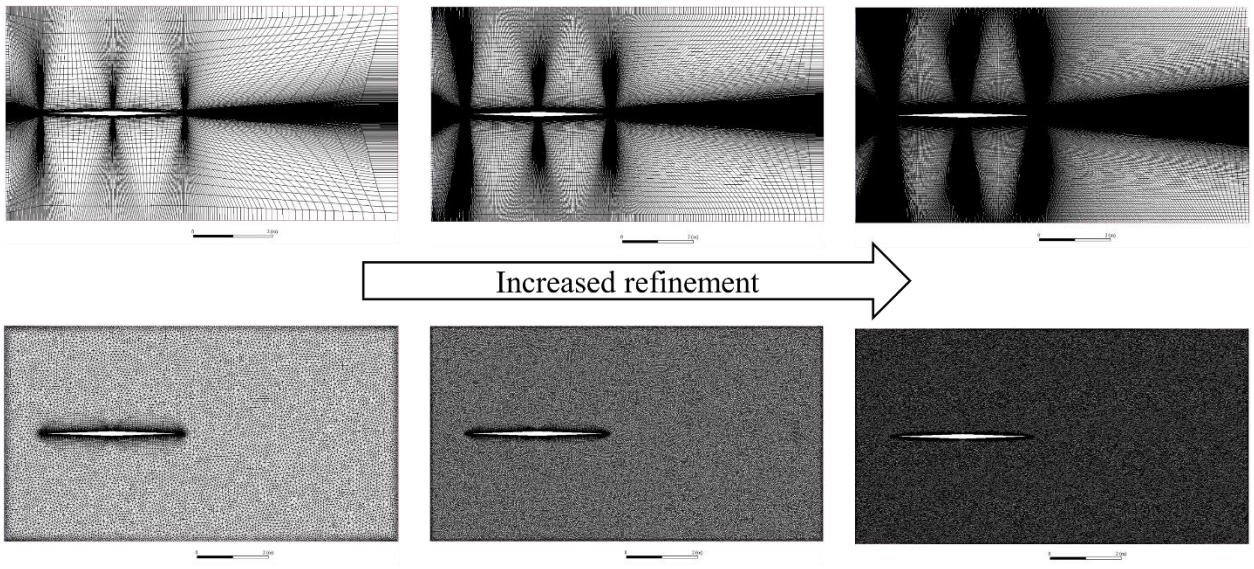

Figure 3: Structured (top) and unstructured (bottom) meshes used

Table 1: Mesh size

Mesh Type	Refinement	Number of Cells
Structured	Coarse	38,808
	Medium	157,608
	Fine	632,208
Unstructured	Coarse	65,304
	Medium	195,976
	Fine	499,534

The number of meshes combined with the two solvers resulted in eight sets of data obtained for each scenario proposed in Chapter 2. All meshes would be used in Fluent, while only the fine meshes would be used in FUN3D.

3.1 Inviscid Comparison

The inviscid case will be compared to theoretical values from shock-expansion theory. Based on shock-expansion, it is expected that flow values will be constant over each surface with a discontinuity at the mid-chord.

The coefficient of drag was calculated using the pressure data over each surface of the airfoil. The pressure values were integrated using the trapezoidal method to obtain a drag value. The coefficient of drag, using the pressure values expected via shock-expansion theory, was expected to be 3.056e-04. The difference values presented in Table 2 are calculated using the percent

difference formula. The average of the calculated coefficients of drag was 3.038e-04, and the data had a standard deviation of 9.210e-07.

$$Percent\ error = \frac{|x_{CFD} - x_{theoretical}|}{x_{theoretical}} * 100 \quad \text{(Eq. 1)}$$

Table 2: Coefficient of drag and errors for inviscid case

Solver	Mesh Type	Refinement Level	CD Value	CD Percent Error, %	Pressure, Average % Error	Temperature, Average % Error
Fluent	Structured	Coarse	3.025e-04	0.5897	0.7823	30.57
		Medium	3.031e-04	0.4072	0.6666	30.32
		Fine	3.037e-04	0.2118	0.5629	12.72
	Unstructured	Coarse	3.047e-04	0.1110	0.7044	12.10
		Medium	3.039e-04	0.1536	0.6198	24.02
		Fine	3.035e-04	0.2640	0.4751	10.14
FUN3D	Structured	Fine	3.056e-04	0.4190	0.2166	4.099
	Unstructured	Fine	3.041e-04	0.0572	1.049	7.628

As expected, the coefficient of drag approached the theoretical value with increased refinement when structured meshes were used with Fluent. It was unexpected to see the error increase with refinement for unstructured meshes. However, since the error is below 1% for all tested combinations of mesh configuration and solver, the values can be considered consistent and convergence is achieved with respect to pressure.

3.1.1 Sensitivity of Mesh Configuration

In order to evaluate the influence of mesh configuration, comparisons were made between meshes of the same level of refinement when used with the same solver. The percent difference between the values was calculated in order to examine sensitivity, where percent difference was calculated using equation 2.

$$Percent\ difference = \frac{|Value_1 - Value_2|}{Value_1 + Value_2/2} * 100 \quad \text{(Eq. 2)}$$

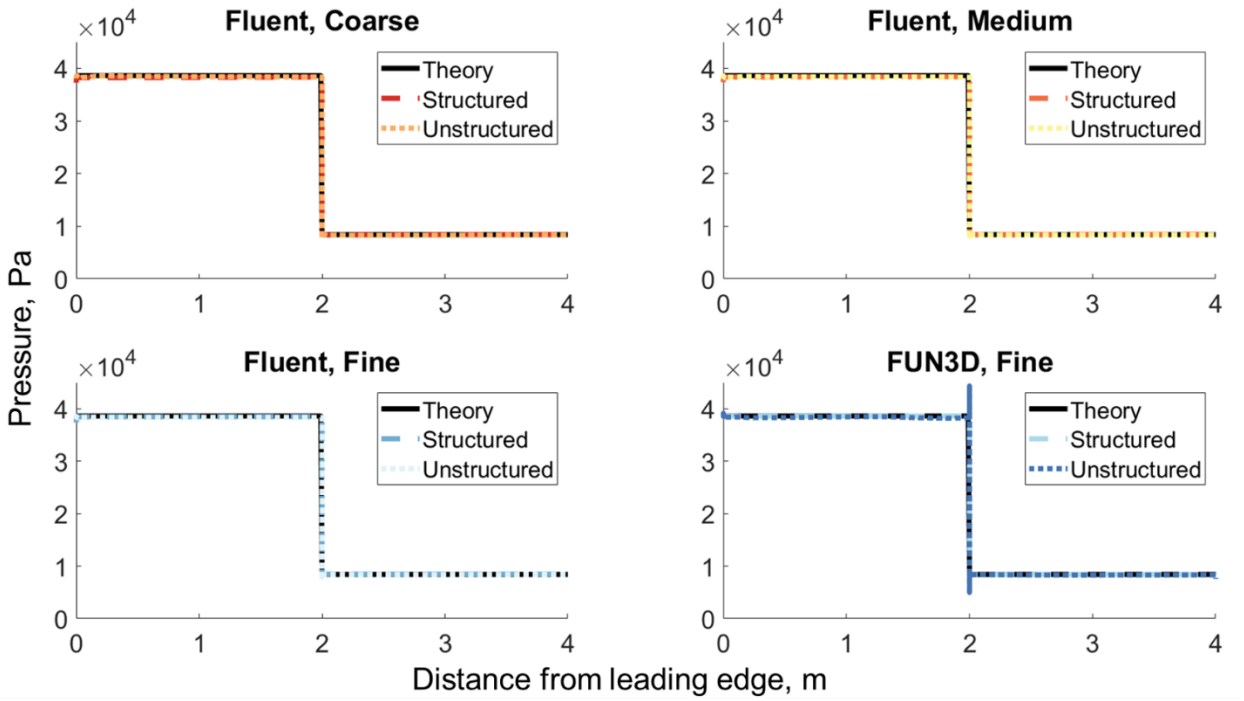

Figure 4: Pressure distribution for inviscid case by mesh configuration

The pressure distribution closely followed the expected shock-expansion values. The largest errors occurred at the mid-chord where there are strong gradients that are difficult to resolve. In contrast, the temperature distributions differed from the expected values.

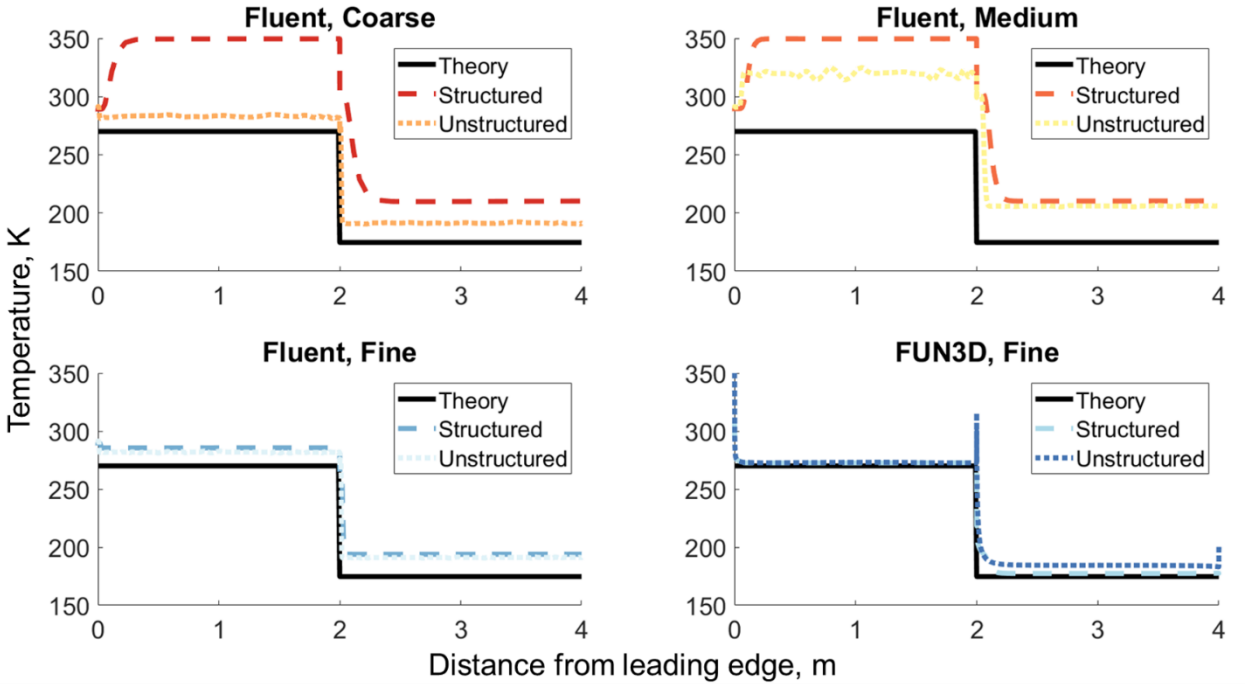

Figure 5: Temperature distribution for inviscid case by mesh configuration

Table 3: Sensitivities with respect to mesh configuration for inviscid case

Solver	Refinement Level	% Difference, CD	Average % Difference, Pressure	Average % Difference, Temperature
Fluent	Coarse	0.7023	0.6722	14.58
	Medium	0.2544	0.5855	4.985
	Fine	0.0523	0.5611	2.189
FUN3D	Fine	0.4753	0.9322	2.902

The strongest sensitivities were seen when comparing the two coarse meshes. Sensitivity for temperature was significantly higher than those of pressure for all levels of refinement, whereas sensitivities with respect to coefficient of drag and pressure were comparable.

3.1.2 Sensitivity of Mesh Refinement

In order to evaluate the affect of refinement, comparisons were made between meshes of the same configuration and solver but of differing refinement levels. Meshes were compared to the finest level of refinement for their respective configurations. Since data was only obtained from FUN3D with one level of refinement, the results presented in this section pertain only to Fluent.

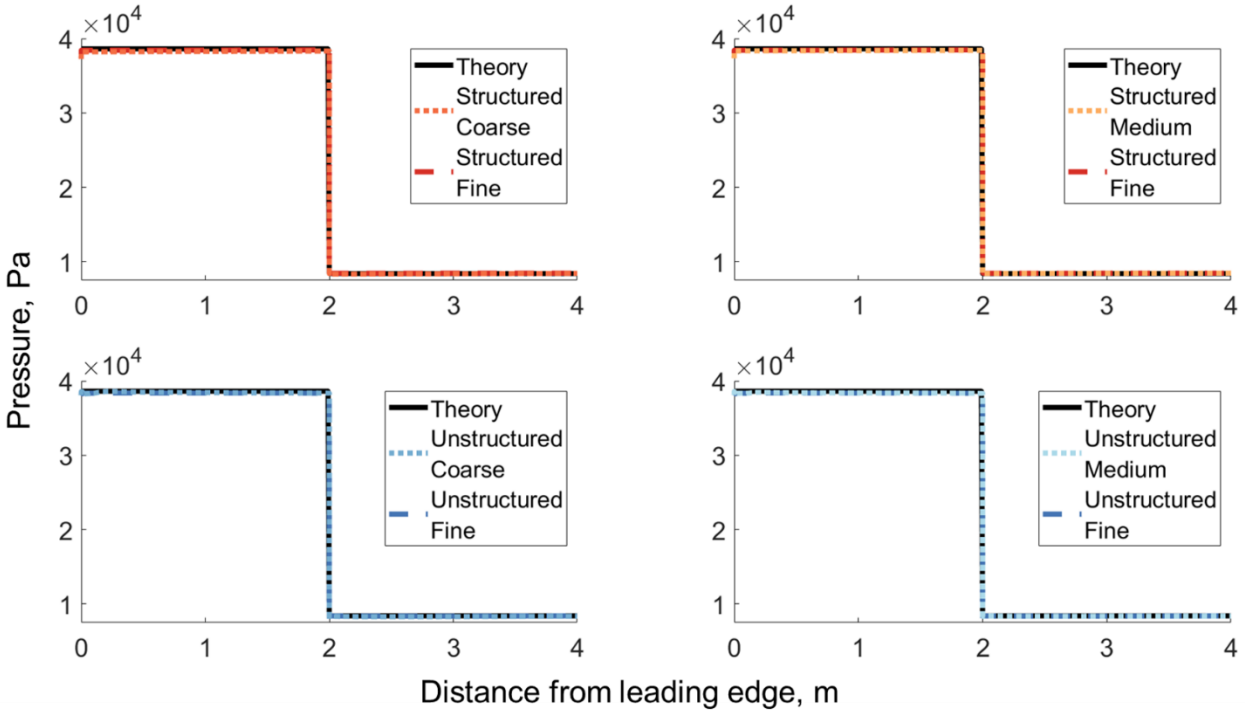

Figure 6: Comparing mesh refinement via pressure distribution for inviscid case

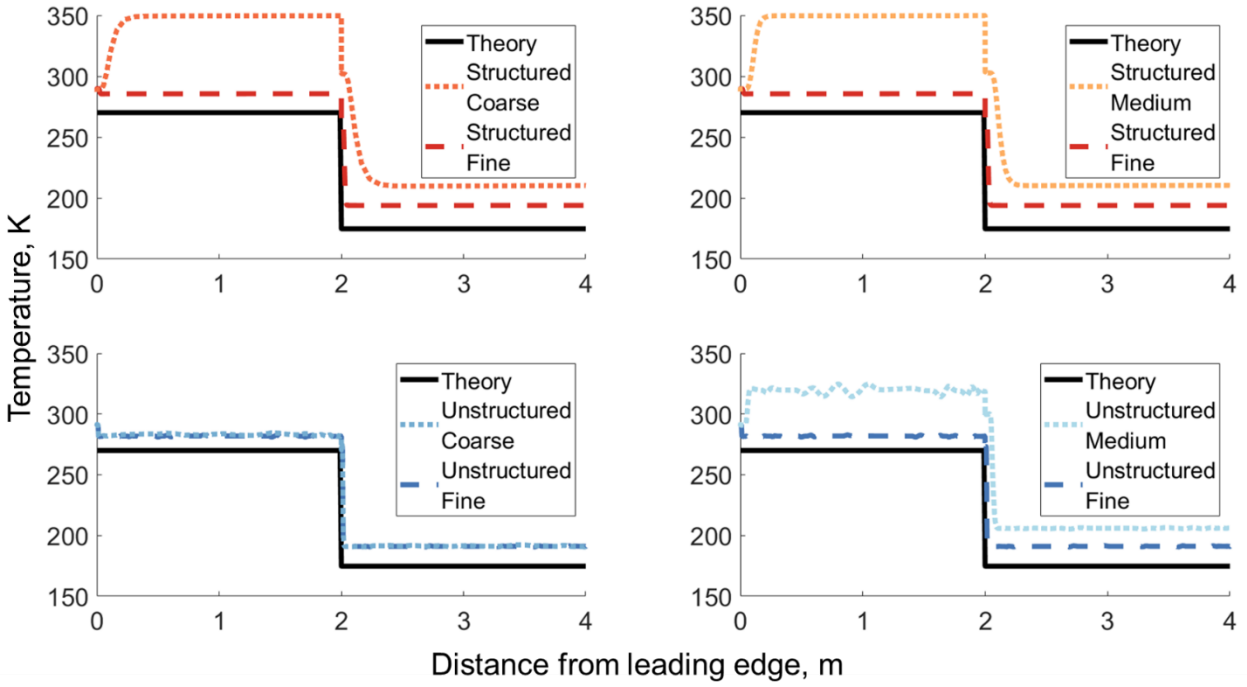

Figure 7: Comparing mesh refinement via temperature distribution for inviscid case

Table 4: Sensitivity with respect to mesh refinement for inviscid case

Mesh Configuration	Refinement Levels	% Difference, CD	Average % Difference, Pressure	Average % Difference, Temperature
Structured	Coarse Fine	0.3794	0.6520	13.52
	Medium Fine	0.1960	0.1677	13.63
Unstructured	Coarse Fine	0.3753	0.4290	0.3259
	Medium Fine	0.1107	0.1832	10.83

It is expected that differences will decrease with increasing refinement as a converged solution is approached. This was seen for both structured and unstructured configurations with regards to coefficient of drag and pressure. However, difference in temperature distributions increased for both types of configurations, dramatically so for unstructured. This was unexpected, as results tend to improve with increasing refinement.

3.1.3 Sensitivity of Solver

Differences with respect to solver were evaluated using the finest meshes.

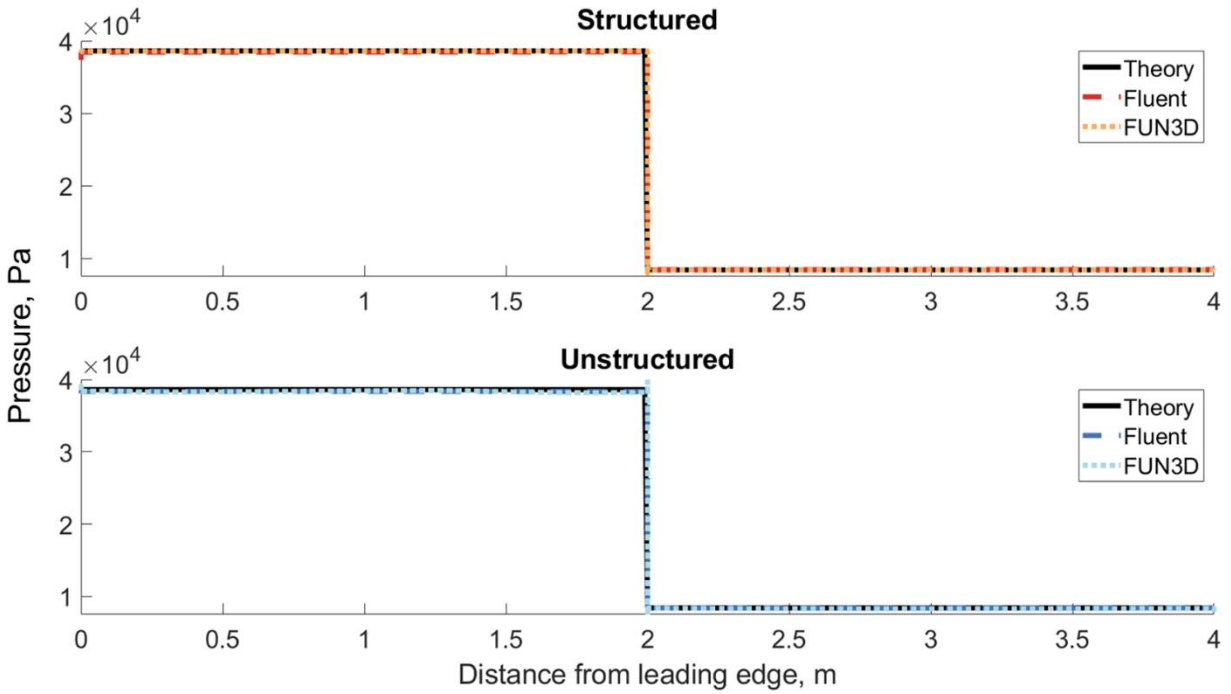

Figure 8: Pressure distribution for inviscid case across solvers

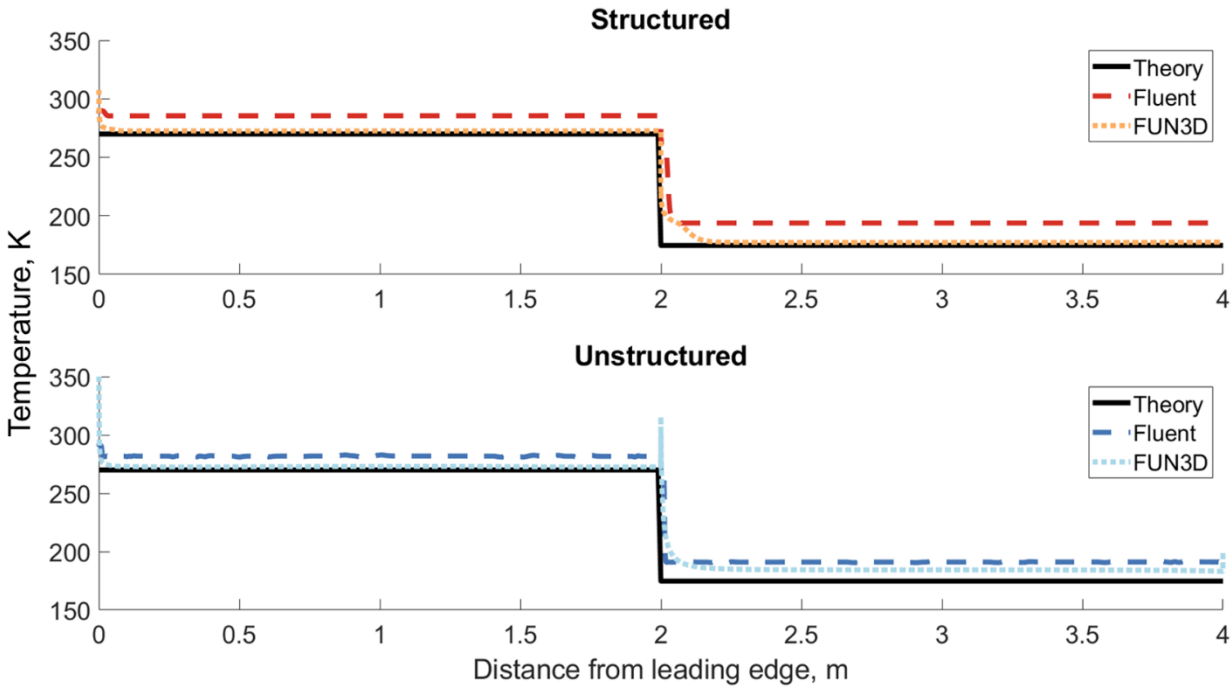

Figure 9: Temperature distribution for inviscid case across solvers

Table 5: Sensitivity for inviscid case with respect to solver

Mesh Configuration	% Difference, CD	Average % Difference, Pressure	Average % Difference, Temperature
Structured	0.6302	0.6700	7.734
Unstructured	0.2072	0.7256	3.945

There is minimal sensitivity for coefficient of drag and pressure distribution across solvers, and moderate sensitivity regarding temperature distribution. This suggests that the implementation of thermal boundary conditions may differ across solvers.

3.2 Adiabatic Comparison

The adiabatic case represents an extreme, as the surface temperature necessary to sustain no heat transfer is significantly higher than is possible. Unlike the inviscid case, there is no theoretical value that can be used for comparison. Thus, comparisons will be made between the CFD results obtained.

Table 6: Coefficient of drag for adiabatic case

Solver	Mesh Type	Refinement Level	CD Value	Maximum Pressure, kPa
Fluent	Structured	Coarse	2.876e-04	261.0
		Medium	2.715e-04	226.1
		Fine	2.685e-04	208.2
	Unstructured	Coarse	2.747e-04	151.0
		Medium	2.685e-04	151.1
		Fine	2.705e-04	151.1
FUN3D	Fine	Fine	3.039e-04	220.4
	Unstructured	Fine	3.037e-04	283.3

3.2.1 Sensitivity of Mesh Configuration

Note that for clarity the pressure distribution has been clipped. Peak values occurred at the leading edge.

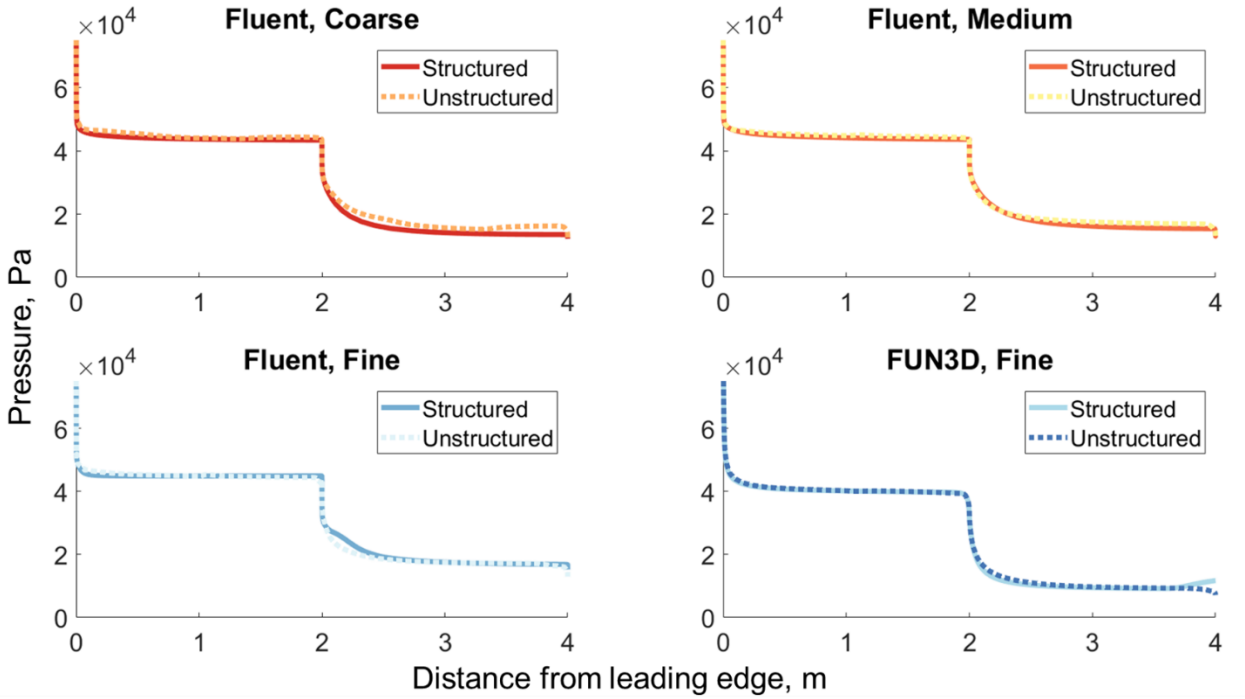

Figure 10: Pressure distribution by mesh configuration for adiabatic wall

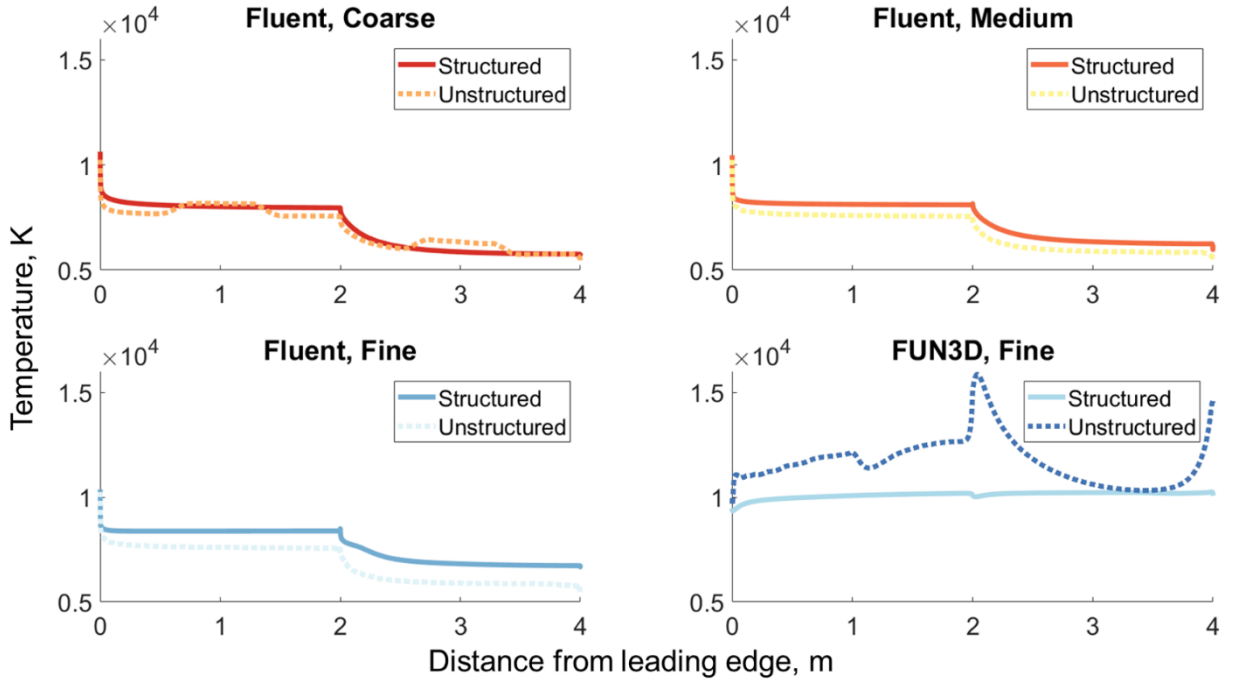

Figure 11: Wall temperature distribution by mesh configuration for adiabatic wall

Table 7: Sensitivity of mesh configuration for adiabatic wall

Solver	Refinement Level	% Difference, CD	Average % Difference, Pressure	Average % Difference, Wall Temperature
Fluent	Coarse	4.585	5.598	4.584
	Medium	1.124	2.889	7.218
	Fine	2.554	3.887	11.62
FUN3D	Fine	0.0660	6.850	21.41

Significantly higher sensitivities are seen for the adiabatic case as compared to those seen in the inviscid case. In general, sensitivities are higher for wall temperature than for pressure, except for the coarsest refinement. It was unexpected to see two orders of magnitude difference in percent difference when comparing FUN3D coefficient of drag and pressure differences. Given how these values are related, it was expected that, like the Fluent results, they would not differ greatly. This difference can likely be attributed to the interpolation scheme employed to calculate percent difference, especially given the 25% difference in peak pressure values.

3.2.2 Sensitivity of Mesh Refinement

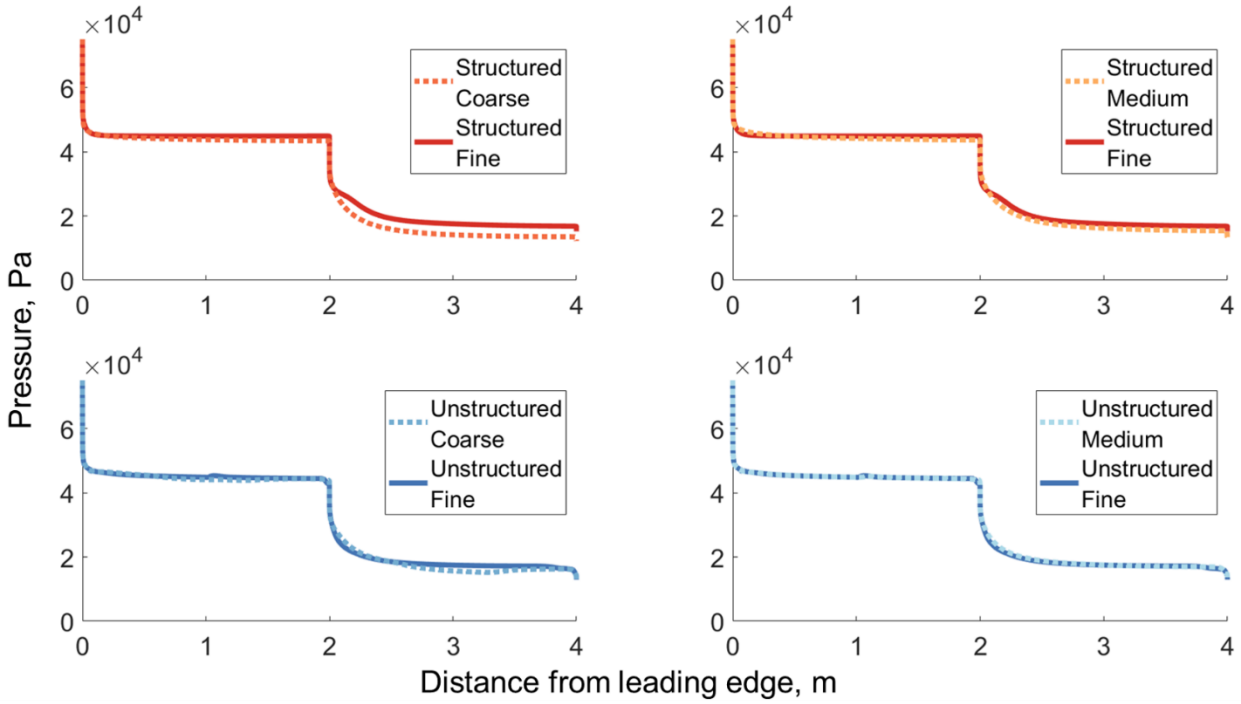

Figure 12: Sensitivity of mesh refinement for pressure distribution of adiabatic wall

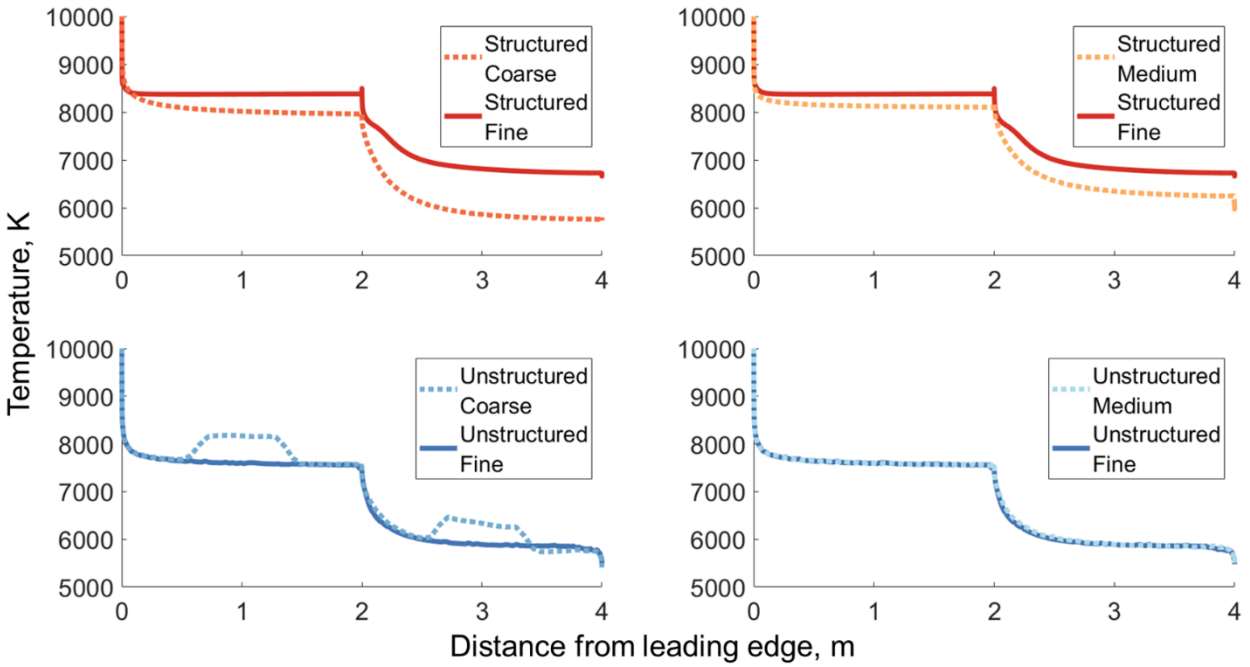

Figure 13: Sensitivity of mesh refinement for pressure distribution of adiabatic wall

Table 8: Sensitivity of mesh refinement for adiabatic wall

Mesh Configuration	Refinement Levels	% Difference, CD	Average % Difference, Pressure	Average % Difference, Wall Temperature
Structured	Coarse Fine	8.682	9.203	7.891
	Medium Fine	2.949	5.014	4.250
Unstructured	Coarse Fine	1.548	2.243	1.281
	Medium Fine	0.7285	1.050	0.3353

Sensitivity decreases with increasing refinement when compared to the finest mesh across all compared variables. While this is expected, the percent differences seen for the medium-fine structured comparison suggests that a converged solution has not been obtained for the structured mesh configuration. In contrast, with differences near or less than 1%, convergence may be considered to have been obtained for the unstructured meshes.

3.2.3 Sensitivity of Solver

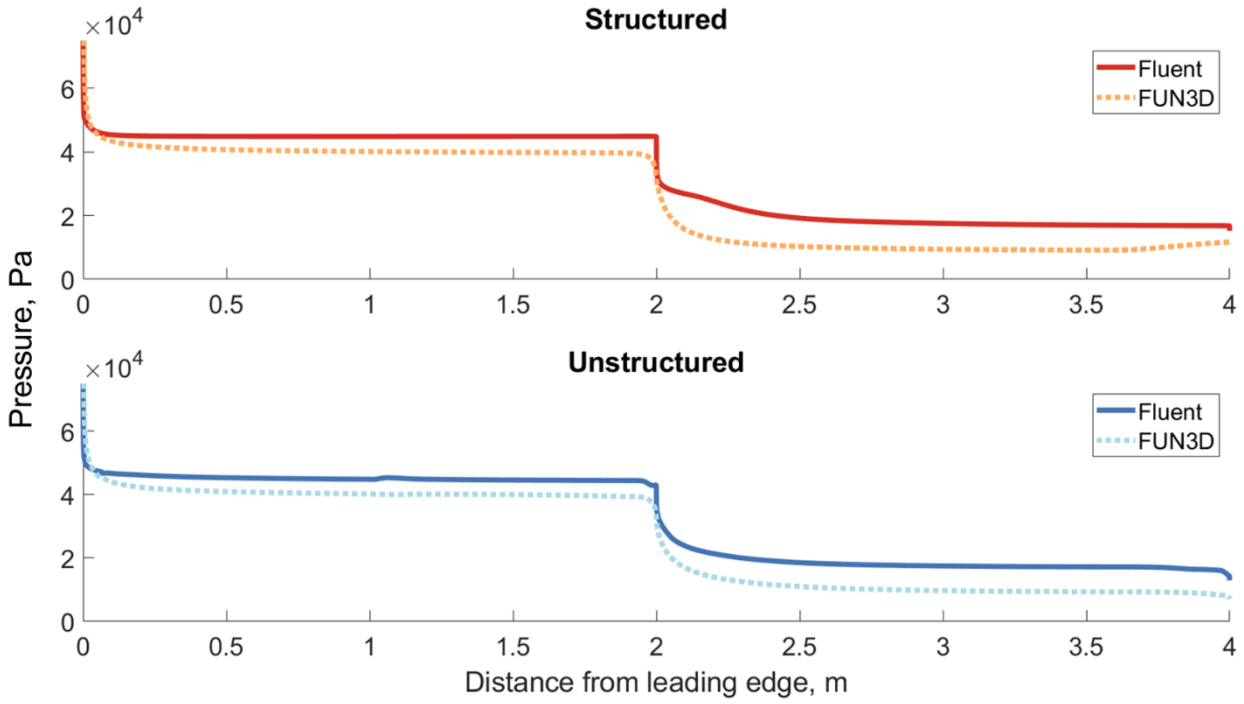

Figure 14: Pressure distribution by solver for adiabatic wall

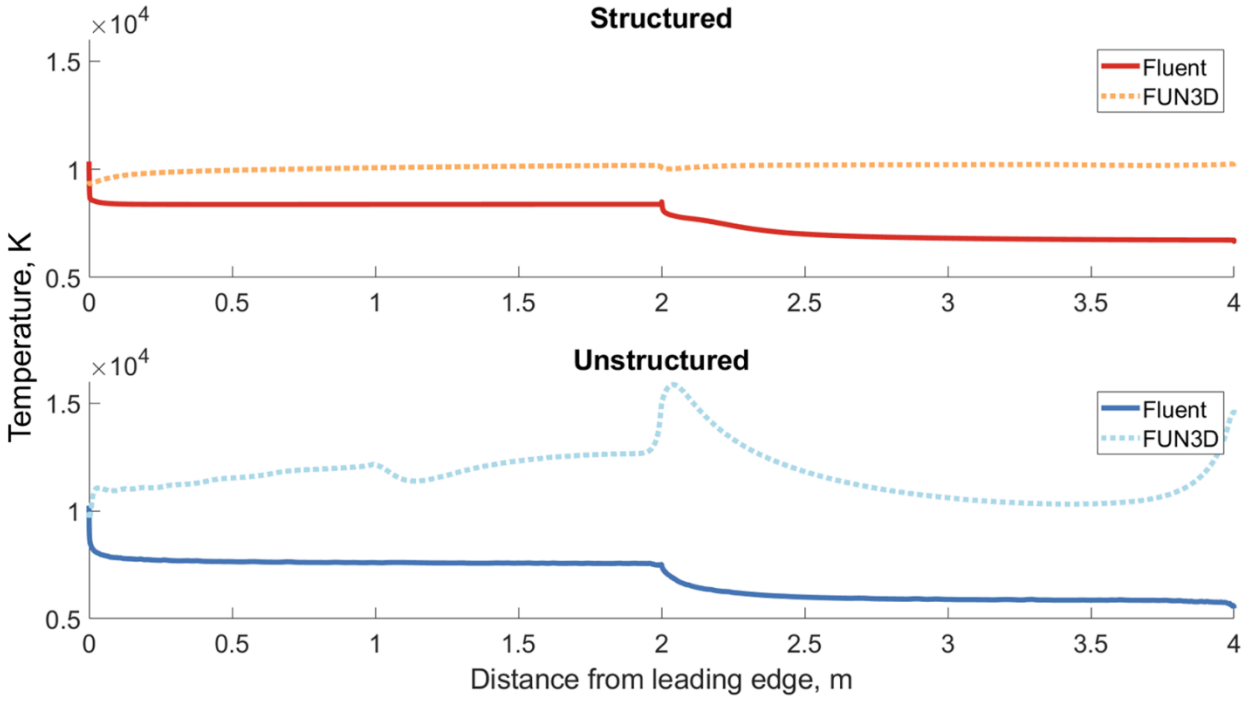

Figure 15: Wall temperature distribution by solver for adiabatic wall

Table 9: Sensitivity of solver for adiabatic wall

Mesh Configuration	% Difference, CD	Average % Difference, Pressure	Average % Difference, Wall Temperature
Structured	14.18	28.10	24.73
Unstructured	11.57	29.80	56.44

Large sensitivities are seen across solvers when comparing the fine meshes of the same configuration. While the average percent difference for pressure may be influence by the interpolation scheme, causing the large disparity between the differences in coefficient of drag and average pressure, it is believed that these interpolations play a minimal factor when compared to the overall differences seen in Figure 14. The wall temperatures follow different patterns across solvers, leading to the large difference. This further reinforces the idea that thermal boundary conditions may be enforced differently between the two solvers, or that the scheme used has a larger impact of temperature distribution than pressure.

3.3 Isothermal Wall at 300K

Both cases set forward thus far are not realistic; an atmospheric vehicle will always experience viscous effects, and the temperature required to sustain an adiabatic wall at Mach 16 is unobtainable. A far more realistic scenario accounts for the presence of viscous effects while maintaining a cooled wall temperature of 300K. For this case, drag and heat flux become critical quantities contributing to the survivability of the vehicle.

Table 10: Coefficient of drag for isothermal wall at 300K

Solver	Mesh Type	Refinement Level	CD Value
Fluent	Structured	Coarse	3.075e-04
		Medium	3.106e-04
		Fine	3.298e-04
	Unstructured	Coarse	3.105e-04
		Medium	3.095e-04
		Fine	3.104e-04
FUN3D	Fine	Fine	3.017e-04
	Unstructured	Fine	3.006e-04

3.3.1 Sensitivity of Mesh Configuration

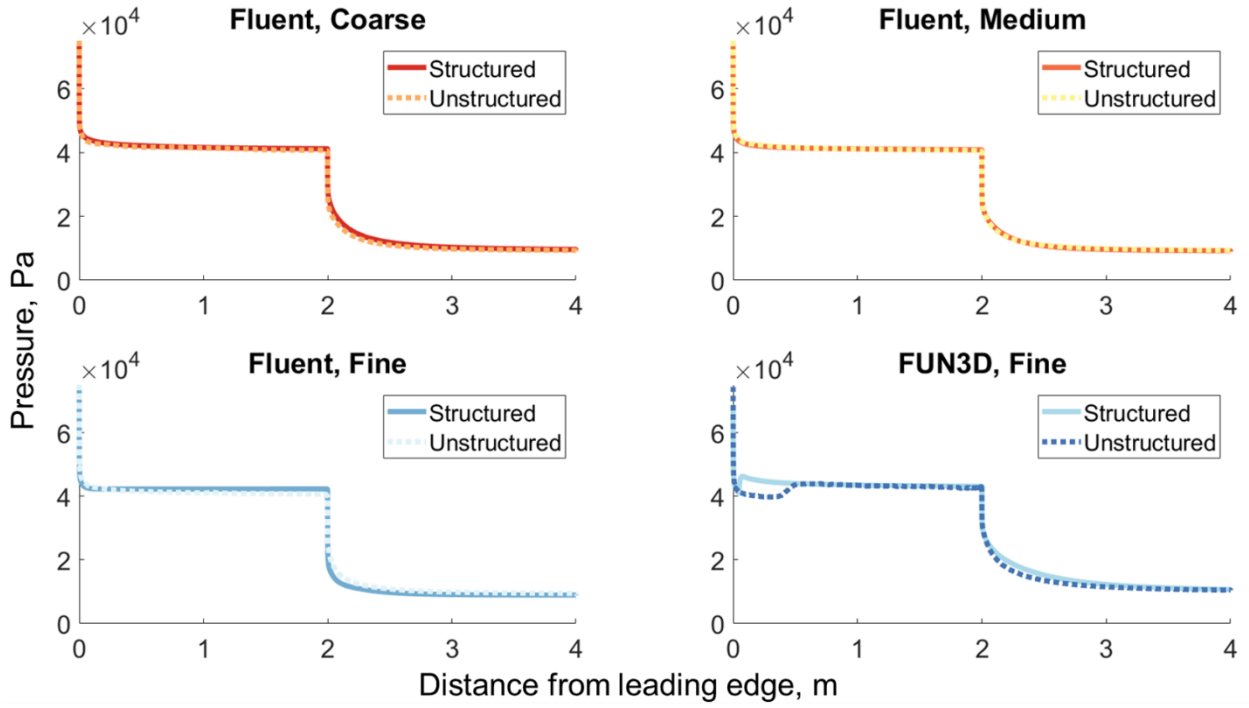

Figure 16: Pressure distribution by mesh configuration for isothermal wall at 300K

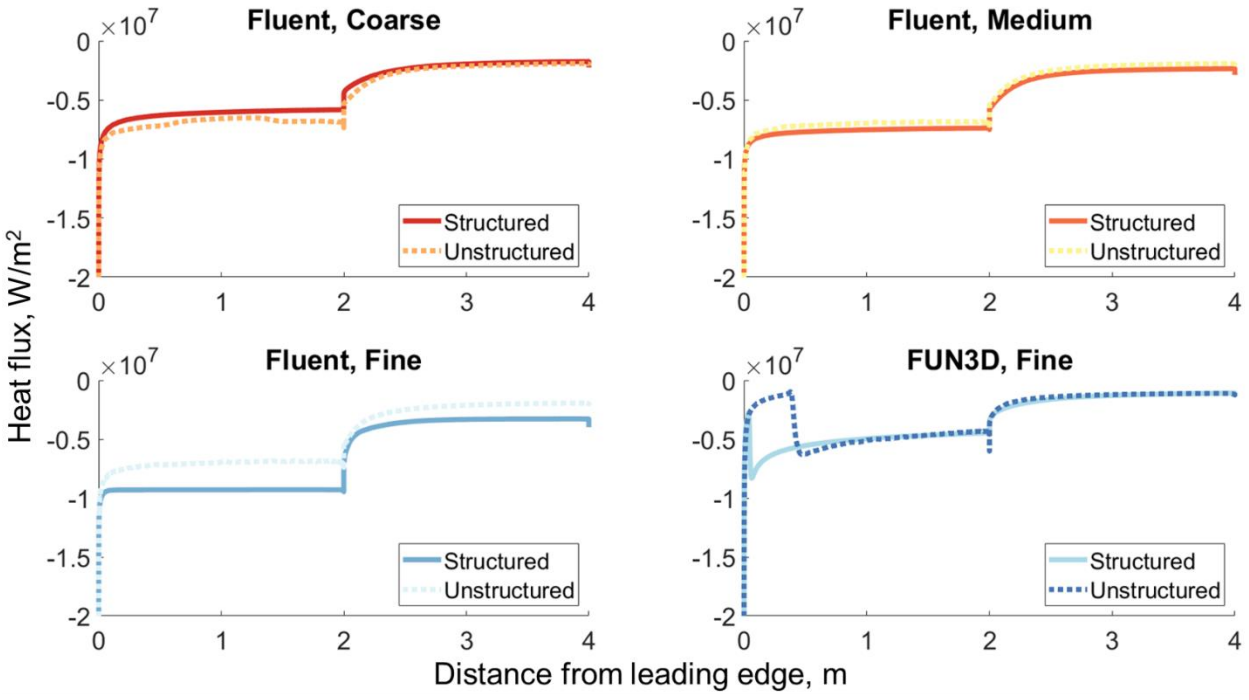

Figure 17: Heat flux distribution by mesh configuration for isothermal wall at 300K

Table 11: Sensitivity of mesh configuration for isothermal wall at 300K

Solver	Refinement Level	% Difference, CD	Average % Difference, Pressure	Average % Difference, Heat Flux
Fluent	Coarse	0.9708	3.858	12.90
	Medium	0.3518	1.219	9.819
	Fine	6.059	6.802	28.97
FUN3D	Fine	0.3887	3.335	15.68

Significant differences are seen with the finest meshes, especially with respect to the heat flux distribution.

3.3.2 Sensitivity of Mesh Refinement

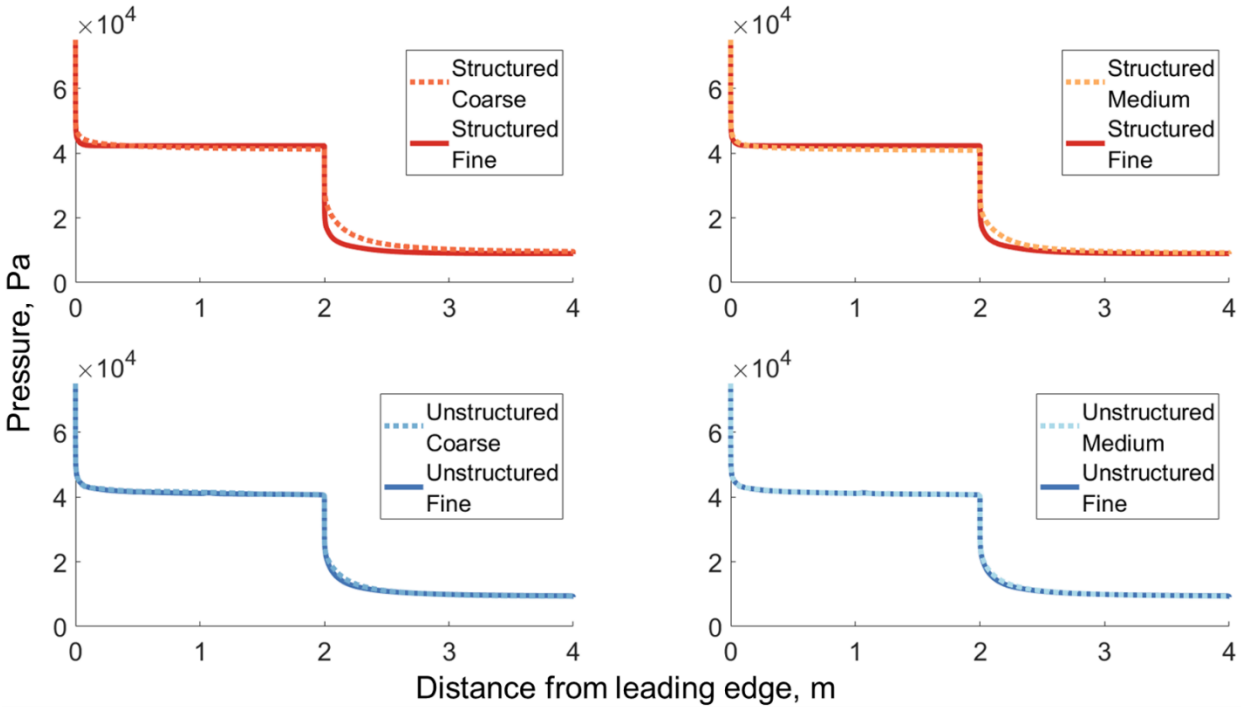

Figure 18: Pressure distribution by mesh refinement for isothermal wall at 300K

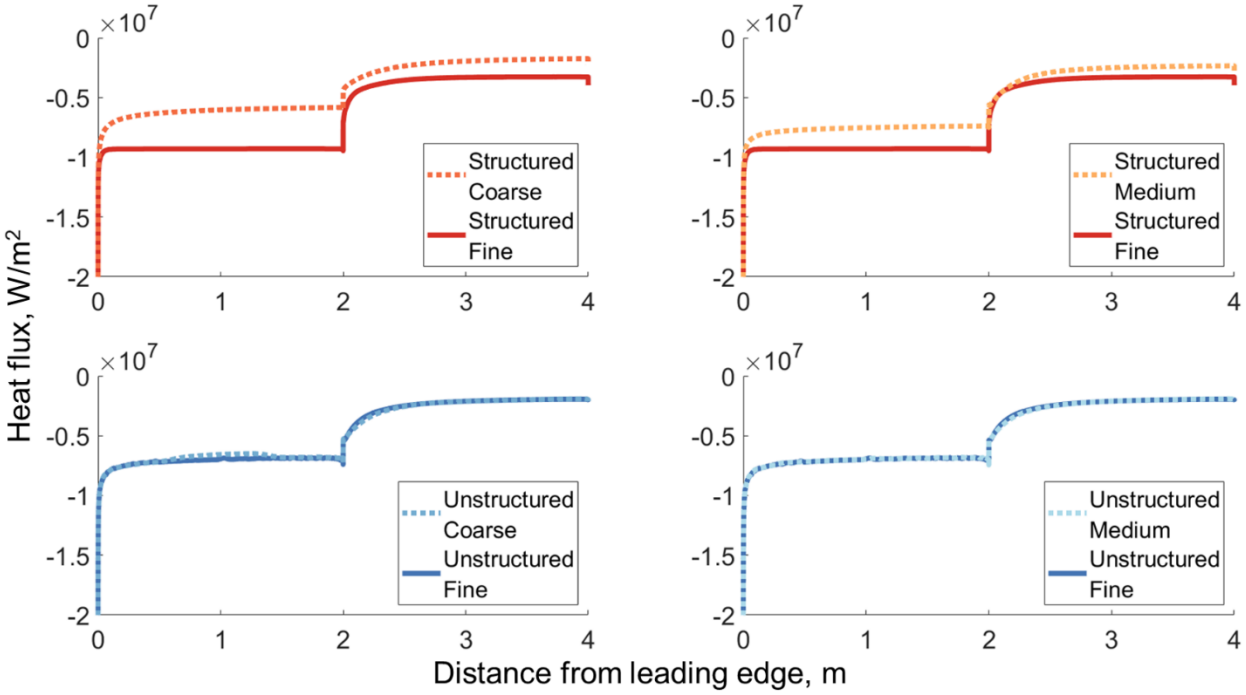

Figure 19: Heat flux distribution by mesh refinement for isothermal wall at 300K

Table 12: Sensitivities by mesh refinement for isothermal wall at 300K

Mesh Configuration	Refinement Levels	% Difference, CD	Average % Difference, Pressure	Average % Difference, Heat Flux
Structured	Coarse Fine	7.022	10.07	40.93
	Medium Fine	6.008	6.448	19.64
Unstructured	Coarse Fine	7.417e-03	1.1330	1.840
	Medium Fine	0.3004	0.8081	0.9479

The unstructured results have negligible sensitivity to mesh refinement. This is in stark contrast to the structured results, which by comparison are significantly more sensitive. However the structured values follow the expected trend of decreased sensitivity with increasing refinement; this is not seen for the unstructured meshes with respect to coefficient of drag.

3.3.3 Sensitivity of Solver

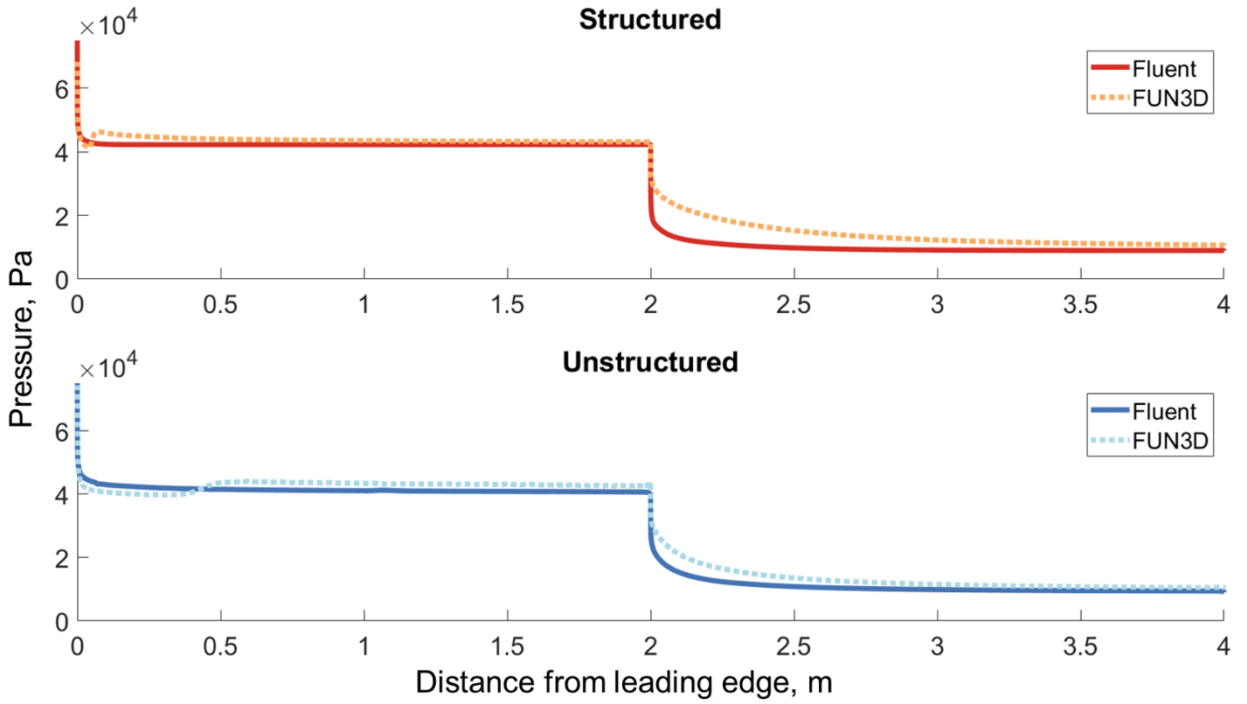

Figure 20: Pressure by solver for isothermal wall at 300K

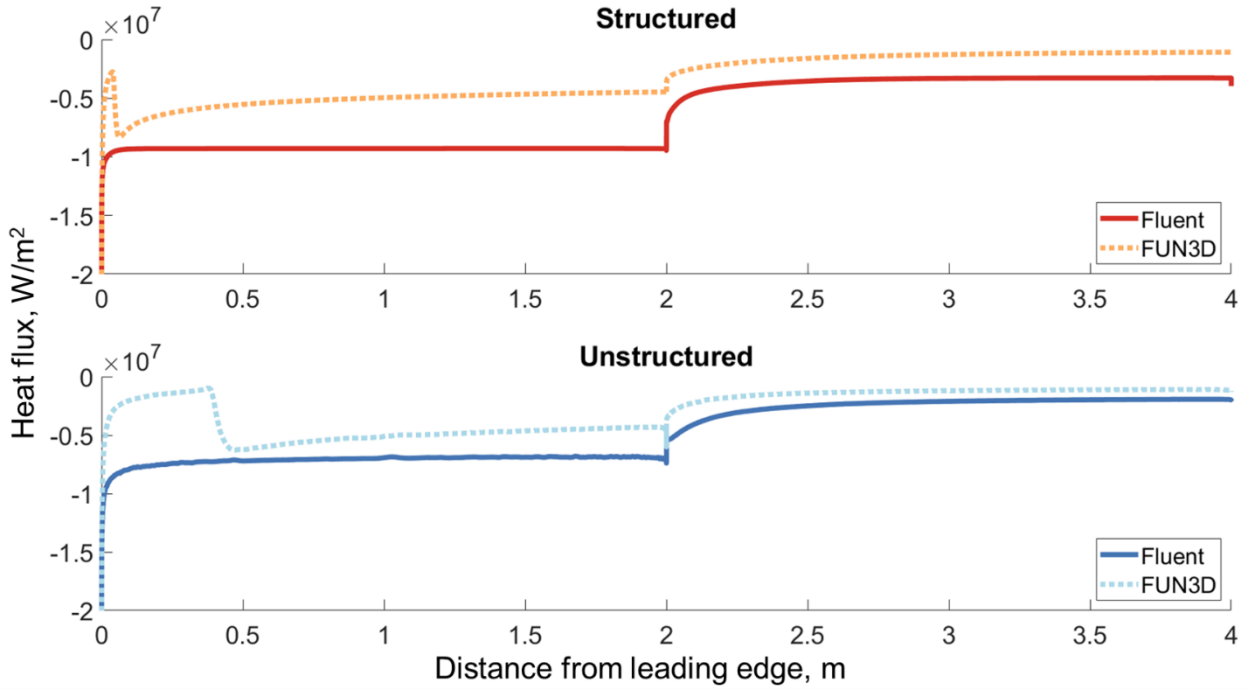

Figure 21: Heat flux by solver for isothermal wall at 300K

Table 13: Sensitivity by solver for isothermal wall at 300K

Mesh Configuration	% Difference, CD	Average % Difference, Pressure	Average % Difference, Heat Flux
Structured	8.894	17.88	70.95
Unstructured	3.228	12.22	55.28

The substantial differences in heat flux would lead to significant differences in heat transfer, which if not calculated properly during the design process would doom a vehicle.

Chapter 4: Conclusion

4.1 Contributions

The greatest sensitivities are seen in the viscous cases, particularly when comparing results obtained with the same mesh using different solvers. This may be attributed the schemes used to solve the governing equations. The Fluent results were obtained using a first-order scheme, whereas FUN3D uses a second-order scheme by default. This could lead to the significant differences between the solvers.

Sensitivity with respect to refinement is an indicator of convergence, as small sensitivities could be attributed to a converged solution. However, for the viscous cases there was still significant differences between adjacent levels of refinement when considering the structured meshes. This highlights a common issue with structured meshes; the levels of refinement required to obtained converged results necessitates both a large number of cells and computational expense.

Further confirmed is the increased refinement required for convergence of temperature-based quantities. Even for the simplified inviscid case, there were large errors with respect to the theoretical temperature values and large differences between the varied parameters. These differences were also seen for the viscous cases, with largest sensitivities seen with respect to mesh type and solver.

The differences with respect to solver can again likely be contributed to the different schemes used. The sensitivity with respect to mesh type however, is not as easily explained. It may in part be attributed to the varying number of points defined on each surface for the varying mesh types. For example, the upper surface of the coarse, structured mesh had 97 nodes, where as the same surface for the coarse, unstructured mesh had 197 nodes. This unintentional increased refinement for the unstructured mesh would be expected to improve the predictive accuracy of the results. This could also contribute to the lower sensitivity seen with the unstructured meshes.

4.2 Future Work

A major limitation of this work is the different schemes used to obtain results. This introduced an unintended fourth variable that would influence the predictive accuracy. The Fluent results should be rerun using a second order scheme to eliminate this variable.

The different number of nodes along the surfaces between structured and unstructured meshes of the same refinement level also influenced the results and limits the validity of conclusions drawn. Different meshes with the same number of nodes along the wings should be used in order to increase consistency between the different mesh types.

Lastly, results should be obtained using the coarse and medium meshes with FUN3D in order to further explore the sensitivities across solvers. There were only two cases that could be compared, in contrast to the four cases when comparing mesh type and refinement levels.

4.3 Summary

Highest sensitivity is seen between differing solvers for the case of hypersonic flow over a double-wedge airfoil. This can be attributed to the different schemes employed by the CFD codes. Differences due to mesh type were higher with respect to temperature and heat flux values than for pressure. Moderate sensitivity with respect to mesh refinement for viscous cases suggested that convergence was not achieved, and that further iterations would be necessary to obtain a converged result.

Appendix A

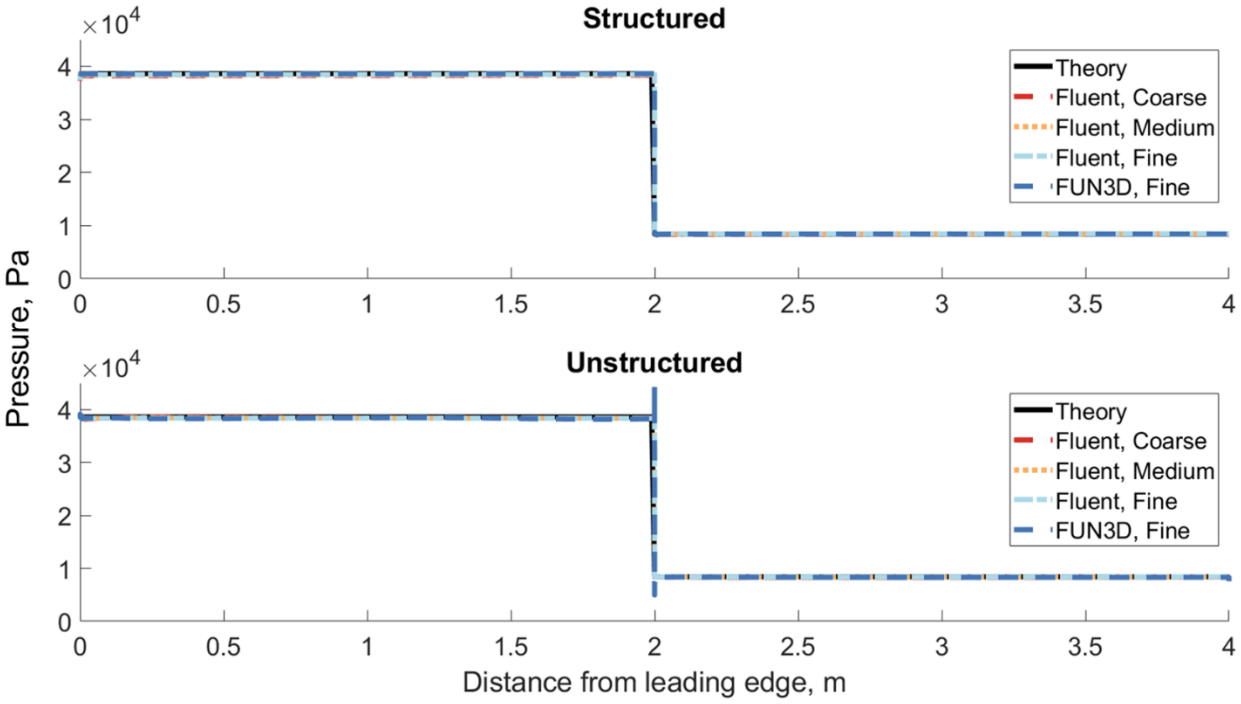

Figure A-1: Pressure distribution for inviscid case by mesh configuration

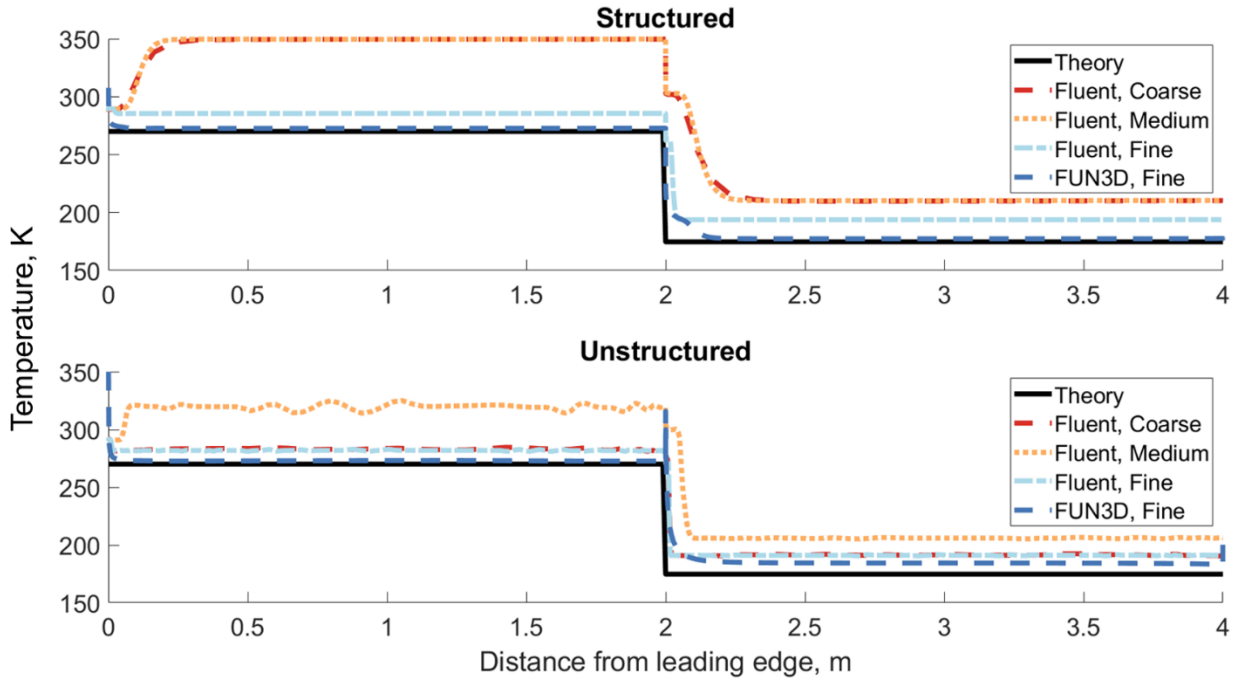

Figure A-2: Temperature distribution for inviscid case by mesh configuration

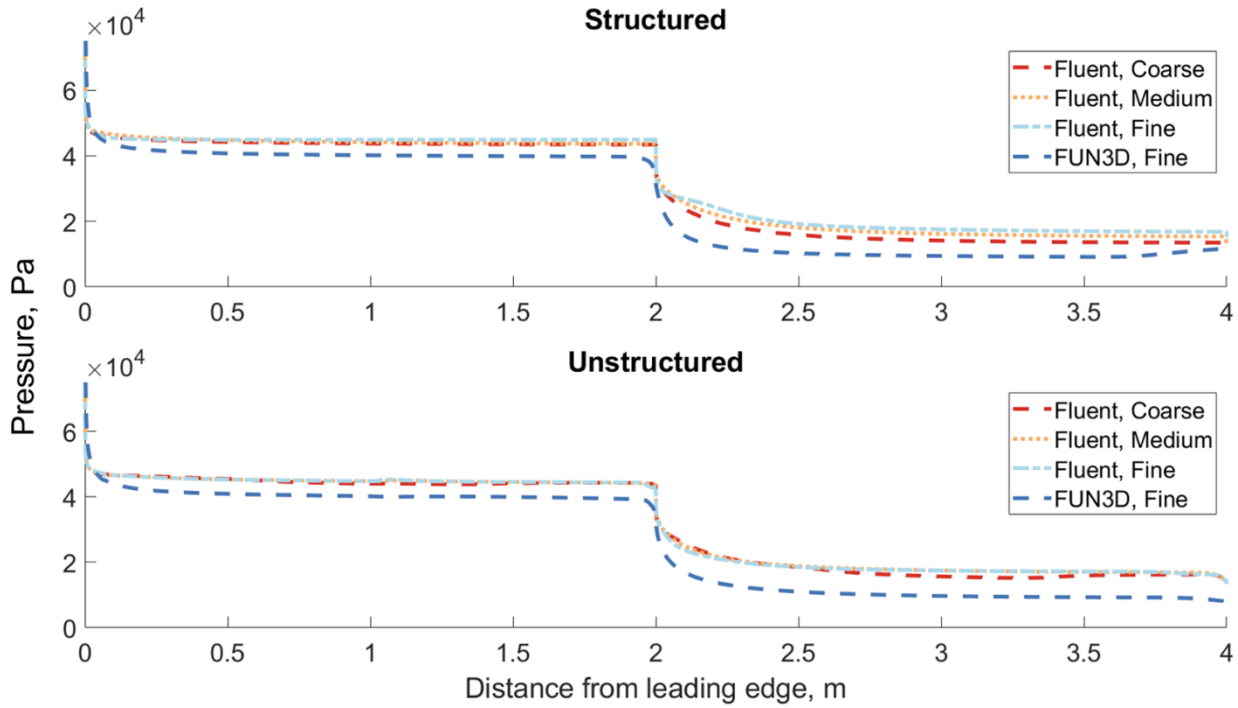

Figure A-3: Pressure distribution for adiabatic case by mesh configuration

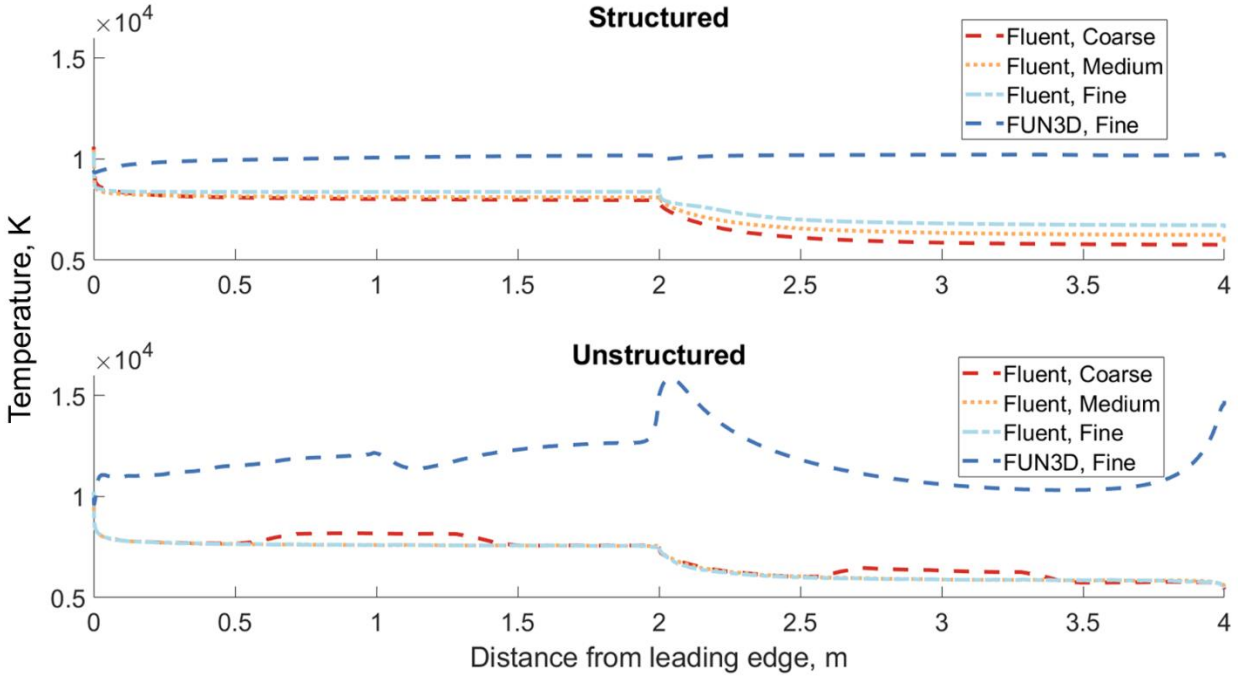

Figure A-4: Wall temperature distribution for adiabatic case by mesh configuration

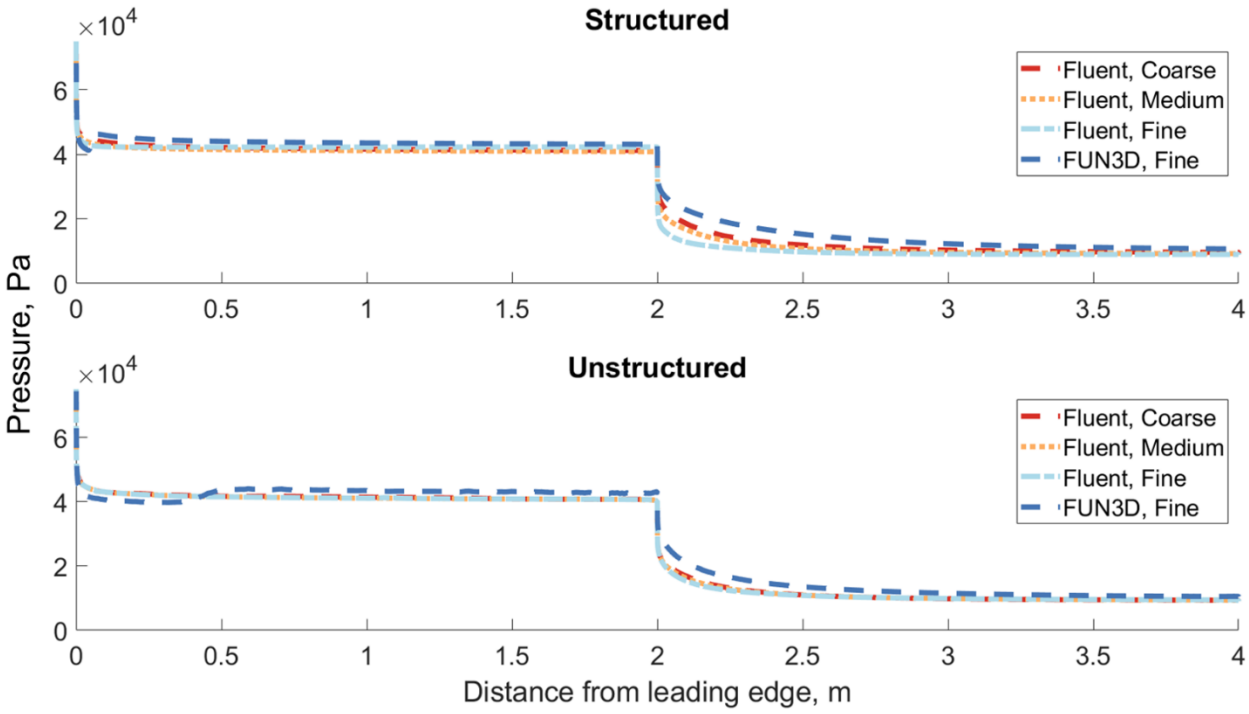

Figure A-5: Pressure distribution for isothermal wall at 300K by mesh configuration

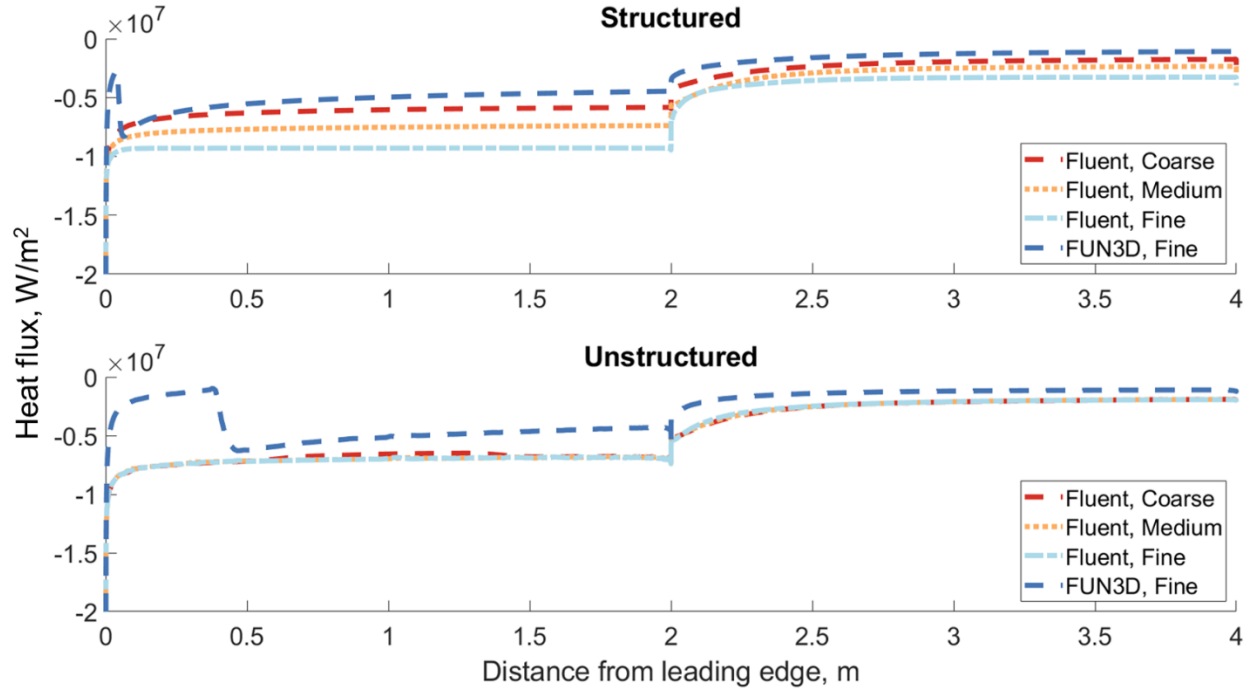

Figure A-6: Heat flux distribution for isothermal wall at 300K by mesh configuration

References

[1]Gaitonde, Datta V., "Introduction to Hypersonic Flow," *Encyclopedia of Aerospace Engineering*, John Wiley & Sons Ltd. DOI: 10.1002/9780470686652.eae035

[2]Dreyer, Emily R., Grier, Benjamin J., and McNamara, Jack J., "Towards Characterization of Relevant Fidelity Modeling of Loads for Maneuvering Hypersonic Vehicles," *2018 AIAA/ASCE/AHS/ASC Structures, Structural Dynamics, and Materials Conference*. DOI: 10.2514/6.2018-1207